On the geometry of fracture and frustration

Koning, V.

6

CURVED CRACK PATHS

6.1 COTTERELL AND RICE THEORY

In the previous chapter, stress intensity factors and kink angles of straight cracks were obtained. To predict the trajectory of a crack, we need to calculate the the stress intensity factors and crack growth direction for curved or kinked cracks. For this we employ the perturbation theory for slightly curved cracks developed by Cotterell and Rice [15]. This theory assumes a small deviation $\lambda(x)$ of a straight crack, as is illustrated in Fig 55. Let $p_n(x)$ and

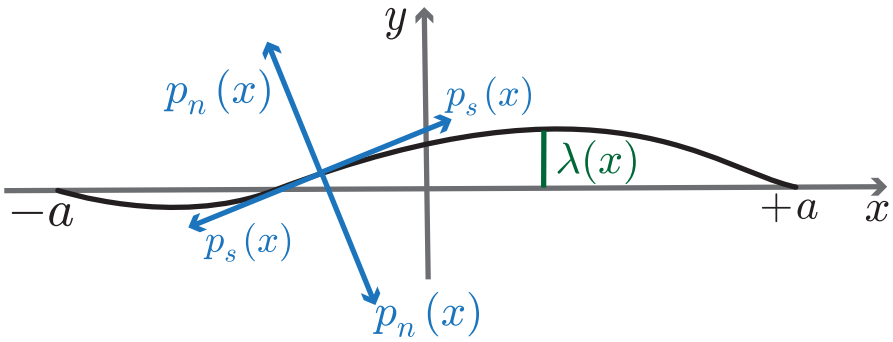

Figure 55: Schematic of a slightly curved crack with crack tips at $x = -a$ and $x = a$, including graphical definitions of $p_n(x)$, $p_s(x)$ and $\lambda(x)$.

$p_s(x)$ denote the normal and shear tractions and primes denote derivatives. The stress intensity factors at the tip at $x = a$ are approximated by [15]

$$K_I = \frac{1}{\sqrt{\pi a}} \int_{-a}^{a} \sqrt{\frac{a+\xi}{a-\xi}} \left(p_n - \frac{3}{2}\omega p_s + \lambda p_s' + 2\lambda' p_s \right) d\xi, \tag{233}$$

$$K_{II} = \frac{1}{\sqrt{\pi a}} \int_{-a}^{a} \sqrt{\frac{a+\xi}{a-\xi}} \left(p_s + \lambda p_n' + \frac{1}{2}\omega p_n \right) d\xi, \tag{234}$$

where $\omega = \lambda'(a)$ is the slope at the tip, which is (to leading order) the angle of the crack tip orientation with the x-direction. If $\lambda = 0$ these expressions reduce to eqs. (214)-(216) for straight

center cracks. For a semi-infinite crack whose (right) tip is located at $x = d$ eqs. (233) and (233) reduce to

$$K_I = \sqrt{\frac{2}{\pi}} \int_{-\infty}^{d} \sqrt{\frac{1}{d-\xi}} \left(p_n - \frac{3}{2}\omega p_s + \lambda p_s' + 2\lambda' p_s \right) d\xi, \tag{235}$$

$$K_{II} = \sqrt{\frac{2}{\pi}} \int_{-\infty}^{d} \sqrt{\frac{1}{d-\xi}} \left(p_s + \lambda p_n' + \frac{1}{2}\omega p_n \right) d\xi. \tag{236}$$

6.2 CRACK PATHS ON A GAUSSIAN BUMP

Based on the stress intensity factors in eqs. (233) and (234), we calculate the kink angle with eq. (186). Next, we grow the crack in the direction specified by the kink angle by a small increment. This process is iterated such that a series of connected line segments forms a crack path. This path approximates a smooth curved crack trajectory provided the length of the increment, Δx, is small enough. We will take $\Delta x = 0.05 x_0$ and show in Appendix D that this choice is sufficient. The only point at which the crack path is not smooth but makes a kink, is at the onset of growth of the pre-existing crack.

We will start with a straight semi-infinite crack in an elastic sheet confined to a Gaussian bump. This pre-existing crack is aligned in the x-direction and its tip is located at $d = -8x_0$. We will vary the initial offset in the y direction, y_{off}. A uniform loading of the entire semi-infinite crack leads to an ill-posed problem, as the stress intensity factors diverge. Instead, we consider a force dipole at $x = x_p$ of magnitude $T \equiv \gamma Y x_0$ (with γ thus a dimensionless number indicating the magnitude):

$$p_n = T\delta\left(x - x_p\right), \tag{237}$$

$$p_s = 0. \tag{238}$$

We will choose $x_p = -10x_0$, thus far away from the bump. Substituting these expressions into eqs. (235) and (236) gives a contribution to the stress intensity factors of:

$$K_I = \frac{\sqrt{2}T}{\sqrt{\pi\left(d - x_p\right)}}, \tag{239}$$

$$K_{II} = \frac{\omega T}{\sqrt{2\pi\left(d - x_p\right)}}. \tag{240}$$

If the slope is positive (negative), *i.e.* the slope $\omega > 0$ ($\omega < 0$), then $K_{II} > 0$ ($K_{II} < 0$) and hence $\theta_k < 0$ ($\theta_k > 0$). Thus the external loading tries to restore the crack to a straight horizontal orientation, with $\omega = 0$.

The curvature has a distinct effect on the crack path. Numerically calculated crack paths for several values of y_{off}, $\gamma = 1$ and $\alpha = 0.5$ are presented in Fig. 56. A zoom of the crack paths around

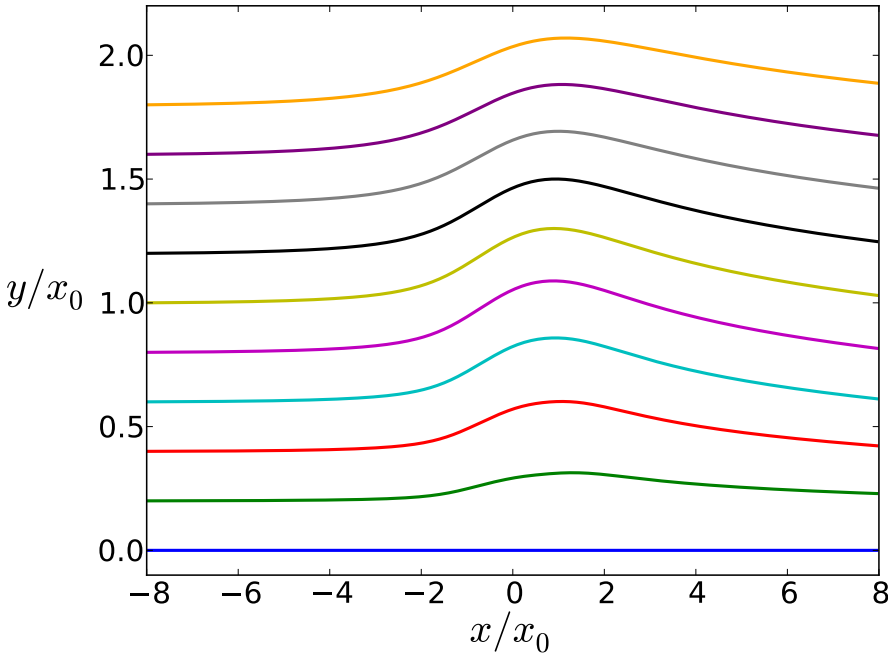

Figure 56: Crack paths for $\alpha = 0.5$ (yellow), $\gamma = 1$, and $y_{\text{off}} = 0$ (blue), $y_{\text{off}} = 0.2x_0$ (green), $y_{\text{off}} = 0.4x_0$ (red), $y_{\text{off}} = 0.6x_0$ (cyan), $y_{\text{off}} = 0.8x_0$ (magenta), $y_{\text{off}} = x_0$ (yellow), $y_{\text{off}} = 1.2x_0$ (black), $y_{\text{off}} = 1.4x_0$ (grey), $y_{\text{off}} = 1.6x_0$ (purple) and $y_{\text{off}} = 1.8x_0$ (orange).

the bump with the x and y on the same scale is shown in Fig. 57. We observe that there is a deflection as the crack approaches the bump. This is can also be inferred from the positive values of ω for negative x (Fig. 58). ω reaches its maximum at $x \approx -0.3x_0$. This corresponds to an inflection point of the crack path. Then ω crosses zero in between $x \approx x_0$ and $x \approx 1.5x_0$ depending on the value of y_{off}, the vertical deflection is maximal and the crack turns. Next is another inflection point beyond $x = 2x_0$, after which the crack eventually attains a horizontal orientation. Interestingly, the deflection is largest when y_{off} is of the order of the width of the

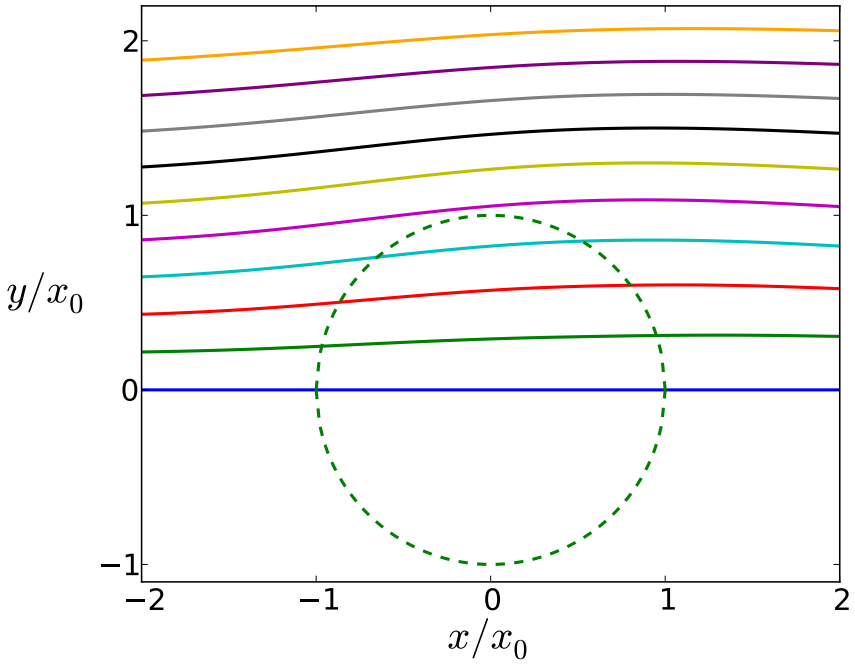

Figure 57: Crack paths for $\alpha = 0.5$ (yellow), $\gamma = 1$, and $y_{\text{off}} = 0$ (blue), $y_{\text{off}} = 0.2x_0$ (green), $y_{\text{off}} = 0.4x_0$ (red), $y_{\text{off}} = 0.6x_0$ (cyan), $y_{\text{off}} = 0.8x_0$ (magenta), $y_{\text{off}} = x_0$ (yellow), $y_{\text{off}} = 1.2x_0$ (black), $y_{\text{off}} = 1.4x_0$ (grey), $y_{\text{off}} = 1.6x_0$ (purple) and $y_{\text{off}} = 1.8x_0$ (orange). Circle $\rho = 1$ in dashed green.

bump. This can be seen from Fig. 59, where we plot the maximal y-deflection Δ as a function of y_{off}.

We can also vary the aspect ratio instead of the initial offset. The crack paths for several values of α are displayed in Fig. 60, $y_{\text{off}} = x_0$ and $\gamma = 1$. The observe that the deflection increases upon increasing the aspect ratio.

6.3 CONCLUSIONS

In conclusion, we have numerically calculated crack paths with Cotterell-Rice perturbation theory. We considered an external normal loading that tends to grow the pre-existing semi-infinite crack horizontally. The curvature-induced stresses are competing with this normal loading. The curvature is responsible for deflecting the crack path, after which it 'goes around' the bump. The magnitude of deflection increases with aspect ratio and is largest when the initial offset is around the width of the bump. Finally, when

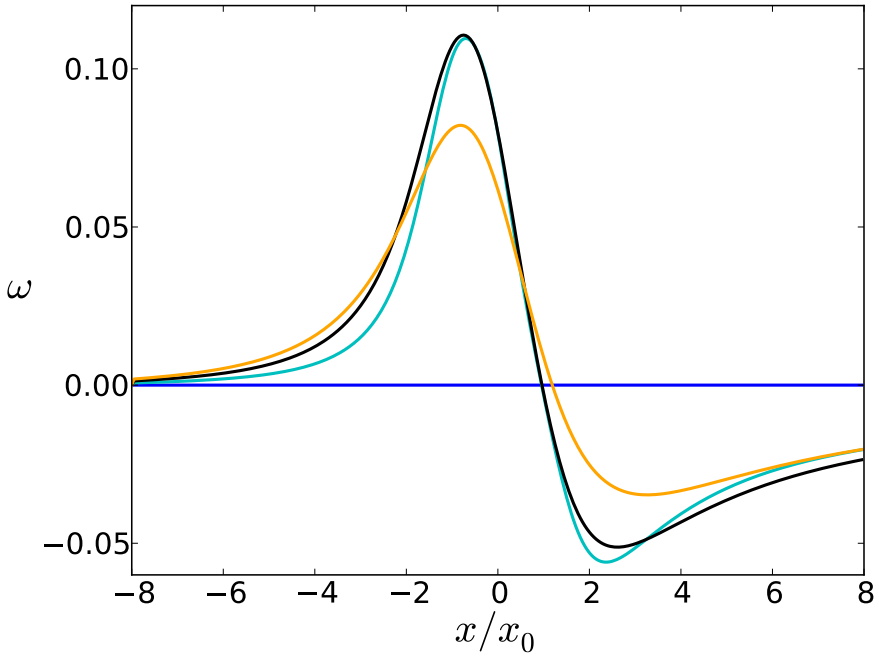

Figure 58: Crack tip angle ω for $\alpha = 0.5$ (yellow), $\gamma = 1$, and $y_{\text{off}} = 0$ (blue), $y_{\text{off}} = 0.6x_0$ (cyan), $y_{\text{off}} = 1.2x_0$ (black) and $y_{\text{off}} = 1.8x_0$ (orange).

the crack tip has past the bump, the crack turns to a horizontal orientation.

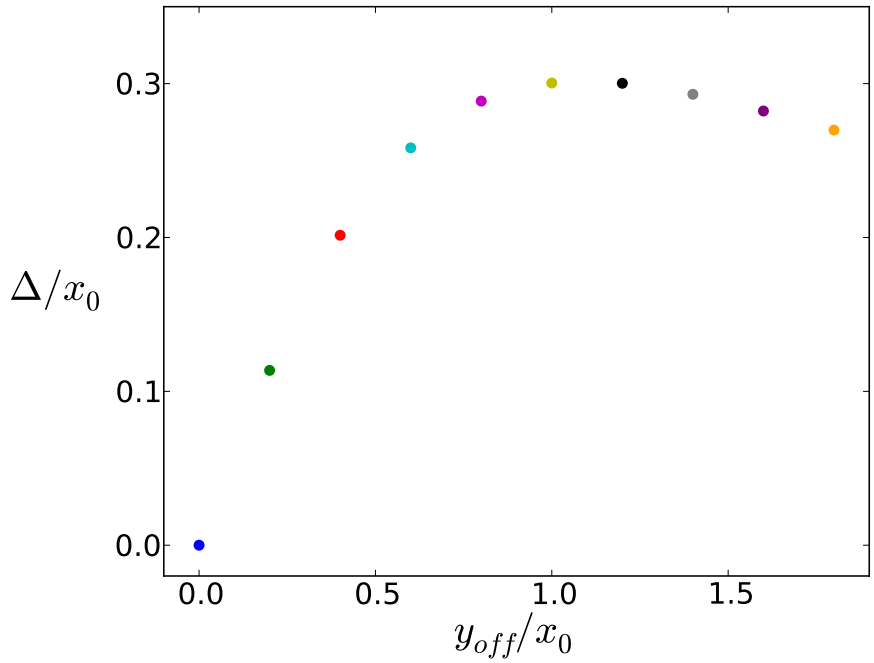

Figure 59: The maximal vertical deflection of the crack path as a function of the initial offset.

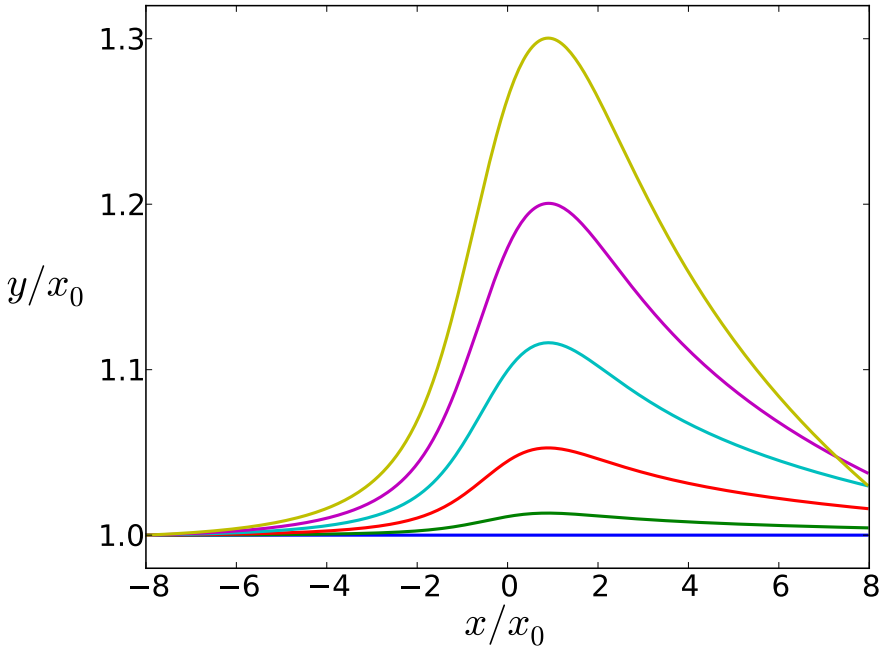

Figure 60: Crack paths for $y_{\text{off}} = x_0$, $\gamma = 1$, and $\alpha = 0$ (blue), $\alpha = 0.1$ (green), $\alpha = 0.2$ (red), $\alpha = 0.3$ (cyan), $\alpha = 0.4$ (magenta) and $\alpha = 0.5$ (yellow).